# Nonlinear dynamics in single-mode optical resonators

J. Danckaert
*Applied Physics Department, Faculty of Applied Sciences, Vrije Universiteit Brussel, Pleinlaan 2, B-1050 Brussels, Belgium*

G. Vitrant and R. Reinisch
*Laboratoire d'Electromagnétisme Microondes et Optoélectronique, Ecole Nationale Supérieure d'Electronique et de Radioélectricité, 23, rue des Martyrs, Boîte Postale 257, 38016 Grenoble, France*

Miltos Georgiou
*Optique Nonlinéaire Théorique, Université Libre de Bruxelles, Campus Plaine, Code Postal 231, B-1050 Brussels, Belgium*
(Received 10 September 1992; revised manuscript received 26 January 1993)

A dynamical analysis of nonlinear optical resonators is performed in the framework of a single-mode formalism in the plane-wave regime, taking the finite response time of the nonlinear medium into account. We demonstrate that analytically solvable generic equations can be derived for the time evolution of the output intensity, in the two limiting cases where the medium's response time is either very large or very small as compared to the cavity buildup time. The stability picture and the characteristic time scales, important for applications in the field of optical information processing, are investigated analytically. This study reveals that a surprising effect may occur where an increase in the material-response time leads to a decrease of the relaxation time of the nonlinear device. This effect is called the speeding-up phenomenon. We also present a numerical study of the full nonlinear dynamics.

PACS number(s): 42.65.Pc, 42.65.Vh

## I. INTRODUCTION

Nonlinear (NL) optical planar resonators have been attracting much attention for some decades now, because of their potential applications in optical information processing and the wealth of physical phenomena they display. Indeed, a host of interesting types of behavior have been observed, depending on the configuration under study (Fabry-Pérot or ring resonators, distributed couplers, multilayered structures, etc.) and on the range of parameters considered [finesse, angle of incidence, finite beam width, type of nonlinearity (absorptive, dispersive, saturating), absorption, material-response time, etc.]. These exciting effects range from bi- and/or multistability, self-pulsing and chaos [1,2], spatial soliton formation [3,4], symmetry breaking, etc. The description of most of these phenomena requires a numerical approach. Nevertheless, simple equations have been proposed to model a wide class of nonlinear planar resonators aiming to derive general analytic laws governing their behavior. For example, Mandel [5] introduced in an *ad hoc* way a generic equation for the transmitted intensity, governing the dynamics of a one-dimensional bistable system in the neighborhood of the switching points. Thereby, he confirmed the existence of critical slowing down in optical bistability, and predicted the phenomenon on noncritical slowing down. These analytical results have been confirmed experimentally, for a variety of bistable systems, including optical ones, both with an absorptive [6] as well as with a dispersive [7] nonlinearity.

As shown by Haelterman, Vitrant, and Reinisch [8], the steady-state response of nonlinear planar resonators, including transverse effects, can be adequately described by a universal modal equation. This approach relies on a single longitudinal-mode assumption in a high-finesse resonator, and its validity has been numerically confirmed, even for resonators with a finesse as low as a few units. A similar equation has been derived from the Maxwell-Bloch equation in a mean-field approach [9]. The same approximation can be used in the time domain leading to a dynamical modal equation [10,11].

We report here results concerning the nonlinear dynamics of planar optical resonators, using this modal approach in the plane-wave regime, and taking a finite medium-response time into account. The theoretical framework is presented in Sec. II. We will discuss in Sec. III under what assumptions a simple equation for the transmitted intensity only can be derived, thereby generalizing the results of Mandel [5] to systems with more than one phase-space dimension. This will also allow us to discuss, among other things, the dependence of the switching dynamics on the Debye time. In Sec. IV, the existence of stable and unstable domains along the stationary S-shaped curve is discussed, as well as the nature of the different solutions and the influence of the Debye time on the characteristic time scales. Finally, Sec. V is devoted to a numerical study of the full nonlinear dynamics, exhibited by these systems, thereby extending the asymptotic results obtained in Secs. III and IV.

## II. DYNAMIC MODAL THEORY

The general dynamical modal equation of a nonlinear optical resonator in the single-mode approximation has been shown to be [10]

 

$$i\partial_t F=\partial_x^2 F+\partial_y^2 F-[i-\eta\Delta+\eta|F(x,y,t)|^2]F(x,y,t)+S(x,y,t)\ . \tag{1}$$

Here, $F(x,y,t)$ is the complex output field envelope function of the transverse spatial coordinates $x$ and $y$ and of time $t$, and $S(x,y,t)$ is the driving field envelope. The time has been rescaled to the cavity buildup time. The longitudinal $z$ coordinate does not appear in the equation because of the single-mode approximation [8]. The detuning $\Delta$ from the closest resonance is scaled to the width of that resonance, such that the finesse does not appear in Eq. (1). The sign of the nonlinearity is given by $\eta$ ($+1$ for self-focusing, $-1$ for self-defocusing). It is important to note that the finesse is the only parameter that limits the range of validity of Eq. (1) in describing the response of planar resonators. This equation can also be derived from the Maxwell-Bloch equations in the single-mode regime for a purely dispersive medium [9,11]. In this paper we will concentrate on the plane-wave case where diffraction phenomena described by the transverse Laplacian in Eq. (1) disappear, reducing Eq. (1) to

$$i\frac{dF}{dt}=-(i-\eta\Delta+\eta|F|^2)F+S\ . \tag{2}$$

In the more general and more realistic case where the medium's response is described by a Debye equation for the nonlinear term, we get the following set of equations [instead of Eq. (2)]:

$$\begin{aligned} i\frac{dF}{dt}&=-(i-\eta\Delta+\eta U)F+S\ ,\\ T_d\frac{dU}{dt}&=-U+|F|^2\ , \end{aligned} \tag{3}$$

where $\eta U$ is the nonlinear term and $T_d$ the nonlinear material-response time.

In order to prepare for both the stability analysis and the discussion of the switching dynamics, we will further simplify Eqs. (3) for small variations of the nonlinear system around the stationary state. The two real variables ($\delta|F|^2=|F|^2-|F_0|^2$ and $\delta U=U-U_0$) are the distances from the stationary states characterized by $F_0$ and $U_0=|F_0|^2$, and can be shown to obey (up to first order)

$$\frac{d^2\delta|F|^2}{dt^2}+2\frac{d\delta|F|^2}{dt}=-\{[1+(\Delta-U_0)^2]\delta|F|^2-2|F_0|^2(\Delta-U_0)\delta U\}\ , \tag{4a}$$

$$T_d\frac{d\delta U}{dt}=-\delta U+\delta|F|^2\ . \tag{4b}$$

Let us note that Eqs. (4) apply whatever the sign $\eta$ of the nonlinearity. It is easy to uncouple these two equations by deriving a third-order linear differential equation for $\delta U$:

$$T_d\frac{d^3\delta U}{dt^3}+(1+2T_d)\frac{d^2\delta U}{dt^2}+\{2+T_d[1+(\Delta-U_0)^2]\}\frac{d\delta U}{dt}=-\{3U_0^2-4\Delta U_0+1+\Delta^2\}\delta U\ . \tag{5}$$

This equation will be the starting point of the analytical results reported in this paper, concerning the switching dynamics (Sec. III) and the stability analysis (Sec. IV).

## III. SWITCHING DYNAMICS

In this section we will see under what assumptions a simple equation for the output intensity can be derived starting from the modal theory. It is useful to recall here that Mandel [5] proposed a simple so-called generic equation [Eq. (3) of Ref. [5] ] in order to describe the switching dynamics of a bistable system. This model was verified for a variety of experimental systems [6,7] [that can be adequately described by a one-dimensional (1D) model] and the analytical results obtained from the generic equation have been shown to be in good agreement with the experimental results. Here, we will generalize the results of Mandel to the three-dimensional system under study here, and thereby we will show under what assumptions such a generic equation can be derived. A quantitative comparison between exact solutions of the modal equation and the analytical predictions will be given. We will also be able to discuss the dependence on the Debye time of important dynamical phenomena such as critical and noncritical slowing down. We will show that Mandel's generic equations can be derived from the modal theory in two limiting cases, namely, (i) $T_d=0$ and (ii) $T_d\gg 1$.

(i) The case $T_d=0$ corresponds to an instantaneously nonlinear medium. The analysis here follows directly from Eq. (2) [or from Eq. (5) by putting $T_d=0$]. Therefrom, the following equation on the intensity $|F|^2$ (for small variations with respect to the stationary state) can be derived:

$$\frac{d^2|F|^2}{dt^2}+2\frac{d|F|^2}{dt}=S^2-[1+(\Delta-|F|^2)^2]|F|^2\ . \tag{6}$$

On the right-hand side (rhs) one recognizes the expression for the stationary response curve, and therefore this member can be interpreted as a measure for the distance of the output intensity from its steady-state value, for a given input field $S$. The existence of the second-order derivative on the left-hand side (lhs) of Eq. (6) is fundamentally due to the fact that the basic Eq. (2) is complex, i.e., that the phase space has two dimensions (phase and amplitude, or equivalently, the parts of the field in phase and out of phase with the driving field). This will be the case for every dispersive nonlinear driven oscillator. Therefore, Eq. (6) is much more general than the context of nonlinear optical resonators in which it has been derived here, and it can be written down for any two-dimensional nonlinear system. If, moreover, slowing down occurs (i.e., in a dynamical regime close to the unstable branch or close to the switching point), $|F|^2$ is a slowly varying function of time, and a kind of slowly varying intensity approximation in the time domain applies. The second derivative on the left-hand side of Eq. (6) can then be neglected, yielding

$$2\frac{d|F|^2}{dt}=S^2-[1+(\Delta-|F|^2)^2]|F|^2\ . \tag{7}$$

Before further simplifying this equation in order to derive Mandel's generic equation, it is convenient to treat first the opposite case $T_d \gg 1$.

(ii) In the limit $T_d \gg 1$, the nonlinear material response is much slower than the cavity buildup process. From Eq. (4b) it follows in this case that the time derivative of $U$ needs to be small (of order $T_d^{-1}$). The time response of the device is then governed by the material-response time, and all the higher derivatives appearing in Eq. (5) can be neglected, yielding

$$T_d[1+(\Delta-U_0)^2]\frac{dU}{dt}=S^2-[1+(\Delta-U)^2]U \ . \quad (8)$$

Equations (7) and (8) have the same structure and will therefore be handled along with same lines. They still do not present analytical solutions, due to the appearance of the third-order term on the rhs. However, since Eqs. (7) and (8) have been derived from a local expansion around an arbitrary fixed point, we introduce little extra errors by further developing the rhs around an arbitrary fixed point $(I_i^*, I^*)$, e.g., one of the switching points. This is done by putting

$$I_i = I_i^* + \lambda \ , \quad (9a)$$

$$I = I^* + x \ , \quad (9b)$$

where $I_i = S^2$ and $I = |F|^2$ [Eq. (7)] or $I = U$ [Eq. (8)]. Developing the rhs of Eqs. (7) and (8) assuming that $\lambda \ll I_i^*$ and $x \ll I^*$, and keeping terms up to second order in $x$, yields

$$\kappa\frac{dx}{dt}=\lambda-ax^2-bx \ , \quad (10a)$$

with

$$\kappa=2 \ \text{ in the case } T_d=0 \ , \quad (10b)$$

or

$$\kappa=T_d[1+(\Delta-U_0)^2] \ \text{ in the case } T_d \gg 1 \ . \quad (10c)$$

The parameters $a$ and $b$ of the rhs of Eq. (10a) depend on the fixed point around which the expansion is made:

$$a=\frac{1}{2}\left[\frac{d^2S^2}{dI_0^2}\right]_{I^*}=-2\Delta+3I^* \ , \quad (11a)$$

$$b=\left[\frac{dS^2}{dI_0}\right]_{I^*}=1+\Delta^2-4\Delta I^*+3I^{*2} \ . \quad (11b)$$

We will now choose $(I_i^*, I^*)$ in the up-switching point, implying that $b=0$ and $a<0$ (all results reported hereafter can be extended to the down-switching point, taking into account that then $a>0$). The stationary solutions in this region are then given by

$$\lambda=ax^2 \Longleftrightarrow x_\pm=\pm\left[\frac{\lambda}{a}\right]^{1/2} \ . \quad (12)$$

We have in fact replaced the S-shaped stationary response curve by a parabola in the vicinity of the switching points (see Fig. 1), $x_+$ being the upper branch (unstable for the up-switching point), $x_-$ being the lower branch (stable for the up-switching point).

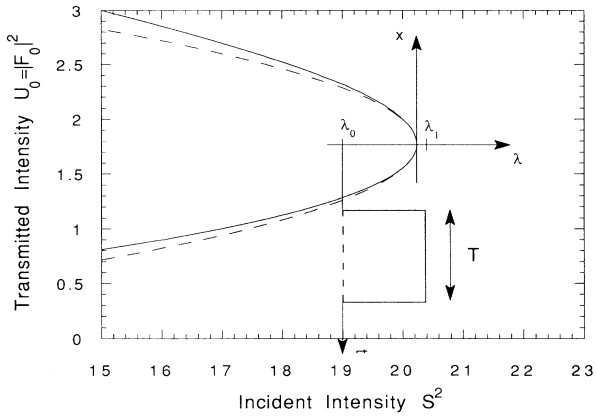


FIG. 1. Representation of the vicinity of the up-switching point, for a detuning $\Delta=5$. The dashed line is the parabolic fit of the S-shaped stationary curve (full line). In order to study the switching dynamics in Fig. 2, the device is initially biased on the lower branch, corresponding to an input irradiance $I_{i,0}=I^*+\lambda_0$ (with in the numerical example here, $\lambda_0=-1.236$, corresponding to $I_{i,0}=19$). Then a pulse of duration $T$ is applied with an irradiance $I_{i,1}=I^*+\lambda_1$ (here $\lambda_1=0.064$, corresponding to $I_{i,1}=20.3$). A numerical solution of the time evolution of the output for these values and different pulse durations is shown in Fig. 2.

Equation (10a) is the equivalent, for dispersive optical bistability, of Mandel's 1D generic equation. Following the procedure in Ref. [5], it can be solved analytically, thus yielding expressions for the critical pulse duration, the switching time, and other lethargic times due to critical and noncritical slowing down. This calculation is presented in the Appendix.

Let us look here at the response of the system to an input pulse with a finite duration $T$, assuming that the device is initially held in a stable state on the lower branch (the situation is schematically depicted in Fig. 1). The initial state is characterized by an input parameter $\lambda_0<0$ on the lower stable branch. During the pulse the system is brought to an input $\lambda_1>0$ barely above the switching point (i.e., $|\lambda_1| \ll |\lambda_0|$). From physical arguments, it is clear that there must be a critical pulse duration $T^*$, separating switching behavior from relaxation back to the initial state. This critical pulse duration can be shown to be given by [see Appendix, Eq. (A9)]

$$T^*=\kappa_1\left[\frac{\pi}{\sqrt{|a\lambda_1|}}-\frac{2}{\sqrt{|a\lambda_0|}}\right] \ . \quad (13)$$

In order to check quantitatively the analytical results, we present numerical solutions of the full nonlinear system [i.e., modal equation and Debye equation, Eqs. (3)] for the case $T_d=10$ in Figs. 2. The critical pulse duration for up switching can be deduced from Fig. 2(a) to lie in the interval $573<T^*<574$. This agrees rather well with the analytical result from Eq. (13), which yields $T^*=560$. We particularly want to draw attention here to the dependence of $T^*$ (and of other dynamical parameters)

on the Debye time through the parameter $\kappa_1 = T_d[1+(\Delta - I^*)^2]$ [see Eq. (A5)], as this could not be included in earlier approaches [5,7]. Indeed, all times that can be calculated will depend on the value of the Debye time $T_d$. Through the same parameter $\kappa$, all times will also depend on the location of the fixed point $(I_i^*, I^*)$ around which the time evolution is studied. This implies, e.g., that the switching times for up and down switching can differ significantly. The critical pulse duration for up switching is seen to be of the order of 570 [Fig. 2(a)], while it is about 59 for down switching [Fig. 2(b)]. This is

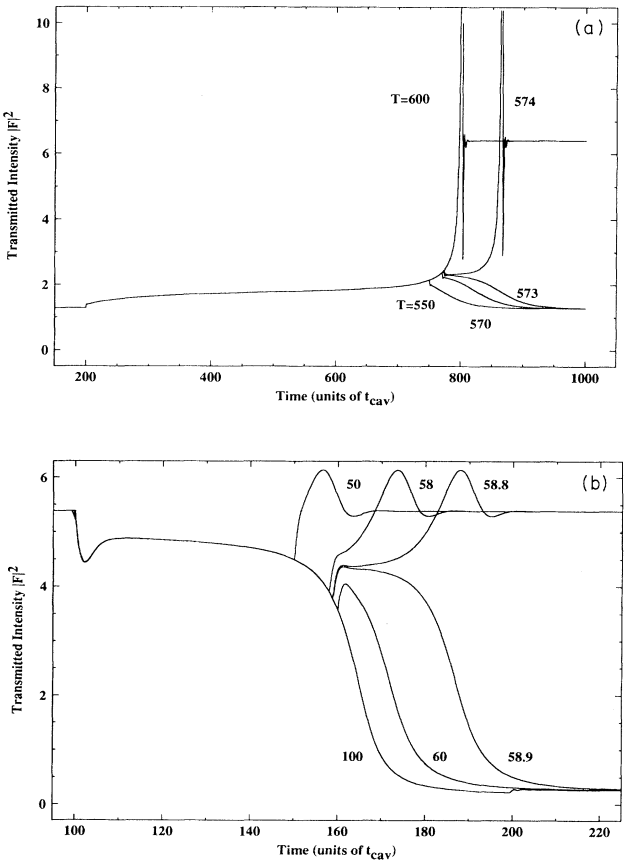


FIG. 2. (a) Up switching for different pulse durations $T$, calculated using an exact numerical procedure solving Eqs. (3), with a Debye time $T_d = 10$. An analytical formulation of the critical pulse duration [Eq. (13)] yields $T^* = 560$, in good agreement with what can be deduced from the numerical results. The large plateau between $t = 200$ and 750 is a manifestation of critical slowing down. The subsequent lethargic behavior for pulse durations close to the critical one is due to noncritical slowing down. (b) In the vicinity of the down-switching point, the same parabolic fit can be used as for the up-switching point (i.e., the values of $|a|$, $|\lambda_0|$, and $|\lambda_1|$ are the same). It can be seen that the critical pulse duration for down switching, and henceforth also the switching time, is very different from the up-switching value (due to the different value of $\kappa$). The analytical expression for the critical pulse duration now yields $T^* = 50$. This still agrees rather well with the numerical result, although the correspondence is less than in the up-switching case. This is because the slowing down is less pronounced here.

a difference of one order of magnitude. Generally speaking, by plugging in approximate expressions for the switching points in $\kappa$, one can verify that the up-switching time will be of the order of $T_d(1+\frac{4}{9}\Delta^2)$ (or slower due to slowing down), while the down-switching time will be of the order of $T_d$ (or slower). For device considerations, it is also interesting to remark that the critical pulse duration for up switching with a Debye time $T_d = 10$ differs by nearly two orders of magnitude from the critical pulse duration for the problem without Debye time [12].

The fact that one is able to derive (under the above-mentioned conditions) a 1D equation describing the originally 3D problem [the phase space of Eqs. (3) is three dimensional] explains the good qualitative correspondence between the analytical results of Mandel and the experiments performed on nonlinear interference filters by Bigot, Daunois, and Mandel [7]. Indeed, the nonlinear interference filters that are used in this work have a slow thermal nonlinearity, and one can thus safely make the assumption $T_d \gg 1$. In the experiments we expect that one could notice the different time scales for the up and down switching, which will also depend on the detuning. Unfortunately for our purposes, Ref. [7] only presents figures for up switching.

To conclude this section, we have derived dynamic generic equations for dispersive optical bistable systems, starting from the general equation coupled with a Debye equation. The main approximation made hereby is a linearization around the stationary state, such that phase and intensity, which are always intimately coupled in dispersive optical bistability, can be decoupled. Furthermore, generic equations can only be applied under conditions of slowing down. Scaling laws, e.g., a pulse area scaling law (see Ref. [5]), critical and noncritical slowing down have thus been established as being generic properties of bistable systems, whatever the system's phase-space dimension may be. A quantitative comparison between the analytical results and exact solutions of the modal equation from which they were derived was made, yielding a good agreement between both. Also, we were able to discuss the dependence of dynamic properties related to switching behavior on the Debye time (in the case $T_d \gg 1$). This parameter induces different time scales for the up- and the down-switching process, furthermore depending on the detuning. We believe that the method outlined above (i.e., decoupling the set of equations by linearizing around the steady-state curve) can be applied to a much larger class of systems than the context of nonlinear optical resonators we have treated here.

## IV. LINEAR STABILITY ANALYSIS

The stability analysis of the modal equation as it stands alone yields the well-known instability of the negative-slope branch of the S curve. The inclusive of the material-response time $T_d$, however, increases the dimension of the phase space to three, allowing for a richer dynamics, as we will now discuss. This stability analysis is done here starting from Eq. (5) dealing with the small variation of the nonlinear term $\delta U$, which, assuming an

exponential time evolution for $\delta U$, results in the following characteristic equation for the exponent $\lambda$:

$$T_d\lambda^3+(1+2T_d)\lambda^2+\{2+T_d[1+(\Delta-U_0)^2]\}\lambda+R=0 ,$$

with (14)

$$R=3U_0^2-4\Delta U_0+1+\Delta^2=\frac{dS^2}{dU_0} .$$

Applying the Routh-Hurwitz criterion, one obtains that the stationary solutions are unstable when one of the two following conditions is satisfied:

$$R<0 , \tag{15a}$$

$$\frac{1+2T_d}{T_d}\{2+T_d[1+(\Delta-U_0)^2]\}<R . \tag{15b}$$

The first inequality [Eq. (15a)] corresponds to the well-known unstable negative-slope part of the $(U_0,S^2)$ stationary response curve and will not be further investigated here. On the contrary, the second inequality [Eq. (15b)] can only be satisfied on the positive-slope portions, and corresponds to a pair of complex-conjugate roots crossing the imaginary axis (i.e., a Hopf bifurcation). The existence of the unstable solutions derived from Eq. (15b) is directly related to the three-dimensional nature of the problem. Inequality (15b) can be solved analytically in order to obtain the unstable domain in the $U_0$ variable (i.e., the stationary output intensity $|F_0|^2=U_0$). Using the expression of $R$ given by Eq. (14) in Eq. (15b), one obtains that unstable stationary solutions only exist if the following inequality, involving only the detuning $\Delta$ and the material-response time $T_d$, is satisfied:

$$D=\Delta^2+4(1-T_d^2)\left[1+\frac{1}{T_d}\right]>0 . \tag{16}$$

This inequality (16) implicitly gives the dependence of the unstable domain boundaries on the material and device parameters. Indeed, the following result can readily be deduced: for a given detuning $\Delta$, instabilities only exist if $T_d$ is smaller than a maximum value $T_{d\max}$, which is plotted as a function of $\Delta$ in Fig. 3(a).

Now, for a given detuning $\Delta$ and provided that $T_d$ lies in the interval $[0,T_{d\max}(\Delta)]$, only a part of the $U_0(S^2)$ stationary response curve is unstable. This part can be analytically calculated, looking at the values of $U_0$ for which the inequality (15b) is satisfied. This procedure leads to an unstable domain that, characterized by the variable $U_0=|F_0|^2$, is given by

$$U_0^- \le \begin{cases} U_0 & \text{if } 0<T_d\le 1 \\ U_0\le U_0^+ & \text{if } 1\le T_d\le T_{d\max} , \end{cases} \tag{17a,17b}$$

where

$$U_0^{\pm}=\Delta+\frac{\Delta\pm\sqrt{D}}{2(T_d-1)} .$$

In other words, for a Debye time in the interval $0<T_d\le 1$, there is an unstable domain extending from a lower boundary called $U_0^-$ to infinity, whereas in the case of $1\le T_d\le T_{d\max}$, the unstable domain has lower and upper bounds $U_0^-$ and $U_0^+$, respectively. Furthermore, $U_0^-$ and $U_0^+$ are both negative if $T_d>1$ and $\Delta<0$, so that in this case the unstable domain vanishes. As a result, for $T_d<1$, instabilities exist in the bistable domain of the stationary bistable characteristic (bistability exists in the case $\Delta>\sqrt{3}$), as well as in the switching domain (where the nonlinearity allows for a self-retuning of the resonator, which is the case if $0<\Delta\le\sqrt{3}$), and even in the limiting domain [where every increase of the nonlinear term induces a decrease of the coupling efficiency of the driving field ($S$) with the resonator field, for $\Delta\le 0$]. In the case $T_d>1$, there exists a finite (bounded) unstable domain or no unstable domain at all, depending on the values of $\Delta$ and $T_d$ (see Table I).

It is possible to characterize more precisely the position of the unstable domain on the $U_0(S^2)$ stationary response curve. Indeed $U_0^-$ is found to be larger than $\Delta$, if $\Delta>0$. The point $U_0=\Delta$ corresponds to the situation where the resonator is self-retuned, i.e., the initial detuning $\Delta$ is compensated by the nonlinearity (the device is on resonance). So, when $\Delta>0$, the inequality $U_0^-\ge\Delta$ shows that the unstable domain is entirely located on the upper part of the $U_0(S^2)$ response curve, i.e., after the retuning or resonance point. In particular, in the case where bistability exists ($\Delta>\sqrt{3}$), the unstable points are located on the upper branch of the bistable loop (the localization of the unstable points is summarized in Table I).

Some important characteristics of the unstable domain are visualized in Fig. 3(b). Indeed, the boundaries separating the stable and the unstable domains are plotted in the $(U_0,T_d)$ plane, for some values of $\Delta$. The analytical results described above are illustrated there. Moreover, one can deduce some interesting results re-

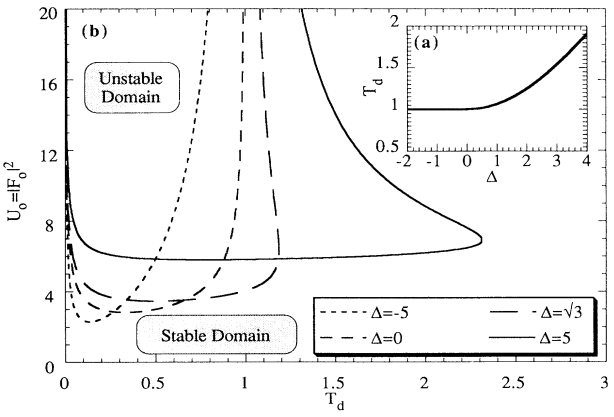


FIG. 3. (a) Minimum value of $T_d$ allowing for the existence of instabilities is plotted vs the detuning $\Delta$. (b) The limit between the stable and the unstable domains is characterized by a critical output intensity $U_0=|F_0|^2$, which is plotted vs the response time $T_d$ of the nonlinear material, assumed to obey a Debye equation. The detuning $\Delta$ is considered as a parameter. Instabilities are due to the existence of two time scales in the system and are found to occur for a bounded domain of $T_d$. The time unit is the cavity buildup time.

TABLE I. Positions of the unstable portions on the stationary response curve (characterized by the stationary output field intensity $U_0$).

| Case | $\Delta<0$ | $\Delta>0$ |
|---|---|---|
| $0<T_d<1$ | unstable for $U_0>U_0^-$ $(>0)$ | unstable for $U_0>U_0^-$ $(>\Delta)$ |
| $1<T_d<T_{d\max}$ | no instability | unstable in the interval $U_0^+>U_0>U_0^-$ $(>\Delta)$ |
| $T_{d\max}<T_d$ | no instability | no instability |

garding the shape of the curve $U_0(T_d)$. Indeed, the system is unstable if $0<T_d<1$ whatever $\Delta$. But the minimum cavity field $U_0$ that can lead to instability diverges when $T_d$ decreases to zero. As a consequence, for a given driving field $S$ related to $U_0$ through the stationary relation $U_0(S^2)$, the resonator is unstable in a window of the material-response time $T_{d\min}<T_d<T_{d\max}$. It is of practical interest to note that the stability property of the stationary solution is very sensitive to the material-response time as this quantity is close to zero: this could be used to measure the material-response time $T_d$.

These results seem in contradiction with numerical results of Ikeda [13] and Abraham and Firth [14], who, considering a full model without the single-mode approximation, showed that instabilities also occur on the lower branch of the bistable curve $U_0(S^2)$. As a consequence we can deduce that instabilities appearing on the lower branch arise due to mode competition, when several modes are simultaneously excited in the resonator. This situation is excluded in our single-mode description applying to high-finesse resonators only. We have shown here that unstable regions located on the upper branch can exist in the single-mode regime, at least in certain regions of parameter space depending on the cavity detuning and the material-response time. This result confirms in a general feature the one obtained by Lugiato *et al.* for a different set of equations describing a single-mode resonator [2]. However, in Sec. V we will see that the full nonlinear dynamics presented by our system here is quite different from the one described in Ref. [2].

It is interesting to look at the solutions of Eqs. (3) that are valid in the vicinity of the stationary solution (first-order expansion) and that yield information on how the system returns to (stable case) or departs from (unstable case) the stationary solution when $S$ is kept constant. Let us call $T_c$ the characteristic evolution time of the system. Then

$$T_c=\{\max[\mathrm{Re}(\lambda_i)]\}^{-1}\ , \tag{18}$$

where $\lambda_i$ denotes the solutions of the characteristic equation (14). The stable and unstable cases correspond respectively to $T_c$ smaller and larger than 0. Besides we notice that simple analytical expressions for $T_c$ can be derived in the following two asymptotic cases $T_d\ll 1$ and $T_d\gg 1$:

$$\text{if } T_d\ll 1 \Longrightarrow \begin{cases} R<1 \Longrightarrow T_c=(\sqrt{1-R}-1)^{-1}\ , \\ R\geq 1 \Longrightarrow T_c=-1\ ; \end{cases} \tag{19a}$$

$$\text{if } T_d\gg 1 \Longrightarrow T_c=-T_d\frac{1+(\Delta-U_0)^2}{R}\ . \tag{19b}$$

Some interesting features concerning the general case can be seen in Figs. 4 where numerical results are presented. The situation considered here corresponds to a detuning $\Delta=3>\sqrt{3}$ so that the stationary response curve shown in Fig. 3(a) is indeed bistable. The hatched region shows the portion of the curve on the positive-slope part that *can* be unstable, depending on the value of the material-response time (see Sec. III). In Figs. 4(b)–4(d) the characteristic time $T_c$ defined above is plotted as a function of the medium-response time $T_d$, respectively for the points $A$, $B$, and $C$ shown in Fig. 4(a). The exact value of $T_c$ is plotted by the full line, while the approximate value, given by Eq. (19b), is shown by the dashed line. The comparison shows that a good agreement between the approximate expression and the rigorous one is indeed obtained for $T_d\gg 1$. The opposite limit $T_d\ll 1$, given by Eq. (19a), only applies for very small values of the Debye time ($T_d<10^{-2}$, not shown in Fig. 4). In Fig. 4(b), for the point $A$ close to the switching point, $T_c$ is negative and $|T_c|$ is much larger than $T_d$. This is related to the critical slowing-down phenomenon close to switching points discussed earlier. In Fig. 4(c), for the point $B$ close to the unstable region, the characteristic time reaches a (negative) peak value for $T_d\cong 0.76$. In the Debye-time domain $0.8<T_d<12$ we observe a very surprising effect, since the characteristic time of the nonlinear resonator decreases when the material-response time increases; moreover, the characteristic time of the system stays much shorter than the response time of the nonlinearity of $T_d>12$. We call this effect the speeding-up phenomenon. This can be seen directly on the dashed line of Fig. 4(c), which corresponds to Eq. (19b). Figure 4(d) is plotted for point $C$, which can be unstable, i.e., $T_c$ is larger than zero in the window $0.26T_d<1.2$. Also here, the speeding-up phenomenon still exists for longer material-response times, similarly to what was observed in Fig. 4(c). To link these results with the discussion of the switching times in Sec. III, it is useful to calculate the characteristic times in the vicinity of the switching points. These are in a first approximation ($\Delta\gg\sqrt{3}$) given by

$$U_0^{\uparrow\downarrow}\cong\frac{\Delta}{3}(2\pm 1)\ , \tag{20}$$

yielding

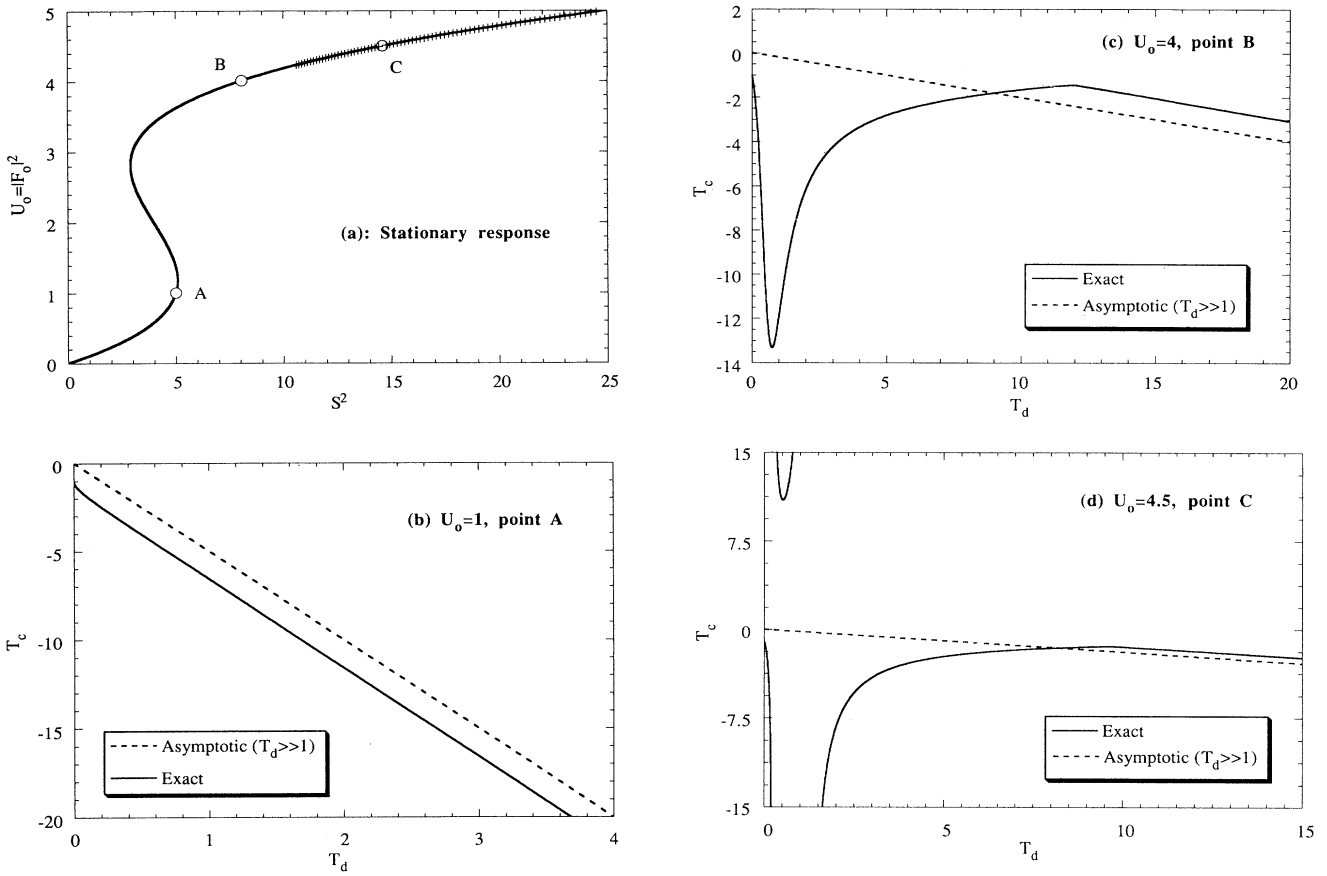


FIG. 4. (a) Steady-state response is plotted (output intensity $U_0=|F_0|^2$ vs the incident intensity $S^2$), for $\Delta=3$ in order to have bistability. The hatched region is the portion of the curve that *can* become unstable, depending on the value of the Debye time. (b) The characteristic response time is plotted by the full line vs the material-response time $T_d$ corresponding to point $A$ of Fig. 2(a). Critical slowing down can be deduced as the characteristic time is much larger than the Debye time. The dashed line shows the asymptotic limit $T_d \gg 1$. (c) Same as (b), but now for point $B$ [Fig. 4(a)]. The speeding-up phenomenon is displayed: (i) the characteristic time $|T_c|$ *decreases* as the Debye time $T_d$ *increases,* and (ii) also in the asymptotic limit ($T_d \gg 1$) the characteristic time is still about five times *smaller* than the Debye time. (d) *Idem* for point $C$. Notice that the system becomes unstable for a Debye time in the interval $0.26 < T_d < 1.2$. Also, here speeding up can be noticed for $T_d > 5$.

$$T_c^{\uparrow} \cong T_d \left[1+\frac{4\Delta^2}{9}\right], \tag{21a}$$

$$T_c^{\downarrow} \cong T_d \ . \tag{21b}$$

These values exactly correspond to the value of $\kappa$ discussed in Sec. III. So, the results presented here are in agreement with those previously obtained from the discussion of the generic equations. They are thus seen to be general, since they do not only apply in the slowing-down case but also in the general case (provided $T_d \gg 1$), however).

## V. NONLINEAR DYNAMICS

The speeding-up phenomenon has been predicted here from a stability analysis that has led to Eq. (5). It can be checked by numerically solving directly the set of Eqs. (3) for suitably chosen initial conditions. An example is shown in Fig. 5 where the cavity intensity $|F|^2$ is plotted versus time for conditions that correspond to point $C$ on Fig. 4(a). The nonlinear system is left free to evolve under a constant excitation starting from an initial condition (on $|F|^2$) that is not very far from the stationary solution. For $T_d=1$, according to Fig. 4(d), the system is unstable. Indeed, in Fig. 5 one sees that the system starts to oscillate and the oscillation amplitude grows at a rate that corresponds to a characteristic time of the order of 10. For $T_d=1.68$, the system is stable [see Fig. 4(d)]. Indeed, in Fig. 5 the system is seen to return to its stationary state after oscillations that are damped with a characteristic time also of the order of 10. For higher value, e.g., $T_d=10$, the system is seen to return more quickly to its equilibrium than it would do having a characteristic time of the order of 1. This surprising property of Eqs. (5) is the speeding-up phenomenon, which could probably be observed experimentally.

As shown by one of the curves in Fig. 5, in the unstable domains the system settles in a self-pulsing regime, a

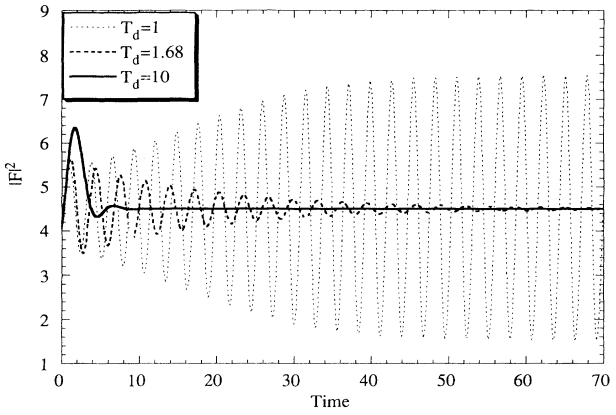


FIG. 5. Nonlinear dynamical response for point $C$ of Fig. 4(a). The output intensity is plotted against time for three different material-response times. The system is unstable for $T_d=1.0$ and stable for $T_d=1.68$ and 10. In the unstable domain a self-pulsing behavior is observed. The response for $T_d=10$ clearly demonstrates the speeding-up phenomenon since the system returns more quickly to equilibrium than for $T_d=1.68$.

behavior typical for a Hopf bifurcation. In Figs. 6(a) and 6(b) the bifurcation diagrams are shown for this particular situation, and for two values of the Debye time, $T_d=1.0$ (infinitely extending unstable domain) and $T_d=1.53$ (bounded unstable domain), respectively. These illustrate that the periodic solutions branching off at the Hopf-bifurcation points are themselves stable, and that the Hopf bifurcations we are dealing with are supercritical.

The occurrence of self-pulsing here needs to be ascribed to the two time scales appearing in the equations, and not to mode competition since the theory was developed here in the single-mode approximation. Contrary to Lugiato *et al.* [2] for a very similar set of equations, and to Yefimov and Shkerdin [15] for another set of equations describing the same physical system, we did not find a bifurcation cascade eventually leading to chaotic behavior. All the periodic solutions we found are themselves stable.

## VI. CONCLUSION

In this paper, we discussed both analytically and numerically the dynamics of nonlinear optical resonators, in the high-finesse limit when only one longitudinal mode is excited. Such resonators can be adequately described by the so-called modal equation, which we considered here coupled with a Debye equation to account for a finite response time of the nonlinear medium.

By expanding this set of equations around the steady state, we found that the three-dimensional problem (in phase space) can be reduced to one effective dimension describing the dynamics in the vicinity of the switching points. In so doing, we generalized Mandel's generic equation describing the switching dynamics of a 1D bistable system to two- and three-dimensional bistable sys-

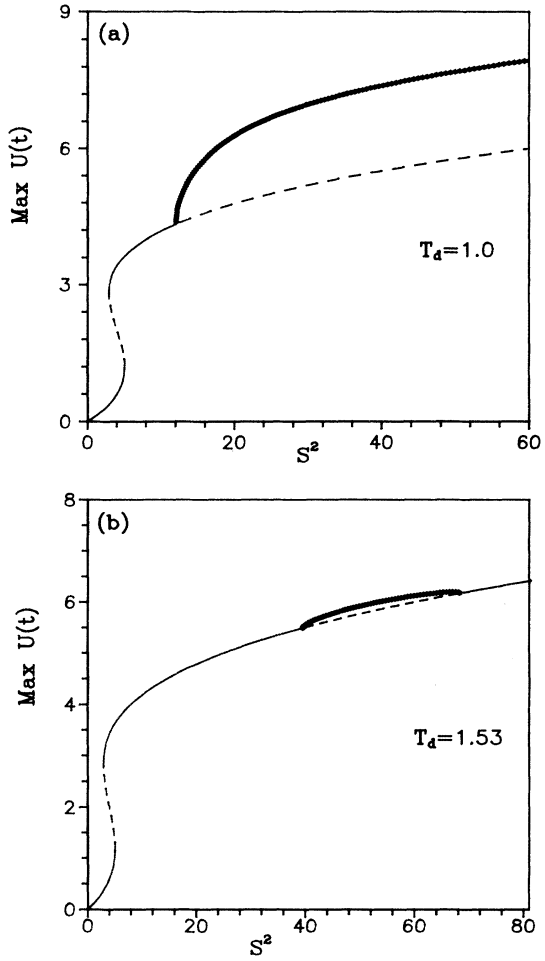


FIG. 6. Bifurcation diagrams, again for a detuning $\Delta=3$ (Figs. 4 and 5) and for two Debye times: (a) $T_d=1.0$, displaying an unstable domain (dashed part) extending to infinity, and (b) $T_d=1.53$, showing a finite unstable region. We always found that the Hopf bifurcations delimiting the unstable regions are supercritical, while the periodic solutions branching off are stable (no further branching points).

tems. We have shown explicitly that this can be done in the limits $T_d=0$ and $T_d\gg1$, under the assumption of slowing down. Although very simple, the generic Eq. (10) can thus be applied to a much larger class of nonlinear optical resonators than was hitherto thought.

Fundamentally due to the presence of two characteristic times, namely the Debye time and the cavity buildup time (taken equal to unity here), a linear stability analysis pointed out the existence of supplementary regions of instability, located above the resonance point of the steady-state response curve. These unstable domains are delimited by supercritical Hopf bifurcations, and their location can be described analytically. The unstable domain extends from a lower boundary to infinity in the case $T_d<1$, moving to infinity in the limit $T_0\to0$, whereas it is finite in the case $T_0>1$, disappearing above a threshold value of $T_d$, depending on the detuning. In the unstable domains, the system presents a regular self-

pulsing behavior. The bifurcation diagrams never showed supplementary branching points where the periodic solution would itself become unstable.

The influence of the Debye time on the switching dynamics (under slowing-down conditions) has been discussed using the generic equation. The Debye time indeed strongly affects the switching time of the device, and furthermore introduces a large difference between the up- and down-switching times. On the other hand, our study of the characteristic time scales with which the system relaxes to or departs from the steady state (far from slowing-down conditions) revealed a surprising effect where the time constant of the device is observed to decrease when the material-response time is increased; we called this the speeding-up phenomenon.

## ACKNOWLEDGMENTS

The authors wish to thank Professor Paul Mandel (ULB) for many stimulating discussions. M.G. (ULB) and J.D. (VUB) acknowledge support from the Inter University Attraction Pole Programme of the Belgian Government. We are also grateful to Professor Irina Veretennicoff (VUB) for many valuable suggestions. Part of this work was performed under a joint collaboration between LEMO and the VUB subsidized by the CNRS (France) and the Flemish Community Government (Belgium).

## APPENDIX

The main result from Sec. III is the derivation of a generic equation [Eq. (10)] governing the switching dynamics from the modal equation (coupled with a Debye equation). The generic equation and its solutions have been discussed in the literature by Mandel and co-workers [5,7] (for a review, see Ref. [16] ). For the sake of completeness, however, we present here the main results, leading to Eq. (13).

The solutions of Eq. (10) can be written as follows.

$$x(t)=\frac{x_-(x_0-x_+)e^{\beta t}-x_+(x_0-x_-)e^{-\beta t}}{(x_0-x_+)e^{\beta t}-(x_0-x_-)e^{-\beta t}} . \quad \text{(A1)}$$

In this expression, $x_\pm$ are the stationary solutions in the vicinity of the up-switching point given by Eq. (12), $x_0$ is the initial value of $x(t=0)$, and the governing time exponent $\beta$ is given by

$$\beta=\frac{\sqrt{a\lambda}}{\kappa} . \quad \text{(A2)}$$

We see that the limit $x(t\to\infty)=x_-$, confirming indeed that $x_-$ is the stable branch of the stationary state (in the vicinity of the up-switching point). However, the solution given by Eq. (A1) diverges when the denominator vanishes. This occurs at a time $t=t^*$, given by

$$t^*=\frac{1}{2\beta}\ln\left[\frac{(x_0-x_-)}{(x_0-x_+)}\right] . \quad \text{(A3)}$$

This time $t^*$ can be associated to the switching time [7] (for times $t>t^*$, the solution is finite again, but is physically irrelevant). Obviously, this divergence can only appear if the argument of the logarithm is positive. In the vicinity of the up-switching point, this is the case when $x_0>x_+$ (as $x_+>x_-$, always). If at $t=0$, $x_0=x_+$, then $x(t)=x_+$, for all times $t$. The unstable branch is seen to act as an separatrix, separating switching behavior from a relaxation back towards the lower branch.

Let us, e.g., look at the response to an input pulse with a finite duration $T$, assuming that the device is initially held in a stable state on the lower branch (see Fig. 1):

For $t=0$,

$$\lambda=\lambda_0<0 \text{ and } x_0=-\left[\frac{\lambda_0}{a}\right]^{1/2} . \quad \text{(A4)}$$

For $0<t\le T$,

$$\lambda=\lambda_1>0 ,$$

with $x(t)$ given by

$$x(t)=-i\Omega\frac{(x_0-i\Omega)e^{i\omega t}+(x_0+i\Omega)e^{-i\omega t}}{(x_0-i\Omega)e^{i\omega t}-(x_0+i\Omega)e^{-i\omega t}} \quad \text{(A5)}$$

with

$$\Omega=\left[\left|\frac{\lambda_1}{a}\right|\right]^{1/2}, \quad \omega=\frac{\sqrt{|a\lambda_1|}}{\kappa_1} ,$$

where $\kappa_1$ is in good approximation given by $T_d[1+(\Delta-I^*)^2]$.

For $t>T$,

$$\lambda=\lambda_0 ,$$

with $x(t)$ given by

$$x(t)=\frac{x_-[x(T)-x_+]e^{\beta(t-T)}-x_+[x(T)-x_-]e^{-\beta(t-T)}}{(x_0-x_+)e^{\beta(t-T)}-(x_0-x_-)e^{-\beta(t-T)}} \quad \text{(A6)}$$

with

$$x_\pm=\pm\left[\left|\frac{\lambda_0}{a}\right|\right]^{1/2}, \quad \beta=\frac{\sqrt{|a\lambda_0|}}{\kappa_0} ,$$

$$\kappa_0=T_d[1+(\Delta-I^*-\lambda_0)^2] .$$

Physically, it is clear that if the pulse is too short, the device will fall back onto its initial state, where as for a sufficiently long pulse duration, it will switch up. According to the separatrix property explained above, up switching will occur only if $x(T)>x_+(\lambda_0)$. So there must be a critical pulse duration $T^*$, implicitly defined by

$$x(T^*)=x_+(\lambda_0) . \quad \text{(A7)}$$

From Eqs. (A5) and (A7), one finds

$$e^{i\omega T^*}=\pm\frac{(x_0+i\Omega)}{(x_0-i\Omega)} . \quad \text{(A8)}$$

One limit is particularly interesting, namely, the limit $\lambda_1\to 0$ (or, equivalently, $\Omega\to 0$), while $|\lambda_0|\ll|\lambda_1|(x_0^2\gg\Omega^2)$, i.e., for a pulse bringing the device barely above

the up-switching point. It yields the following equation for the critical pulse duration $T^*$:

$$T^*=\kappa_1\left[\frac{\pi}{\sqrt{|a\lambda_1|}}-\frac{2}{\sqrt{|a\lambda_0|}}\right]. \tag{A9}$$

A divergence with the inverse square root of the pulse height above switching condition ($\lambda_1$) can be noticed. The closer the device is biased above the switching point, the longer the pulse duration must be in order to assure a commutation of the device. This can be interpreted as a *critical slowing down of the critical pulse duration.* The issue of the switching time of the device, once the pulse duration exceeds the critical one, can now also be addressed. It is determined by the time $t^*$ for which the denominator of Eq. (A5) vanishes:

$$e^{2\beta(t^*-T)}=\frac{[x(T)-x_-]}{[x(T)-x_+]}. \tag{A10}$$

If the pulse duration barely exceeds the critical one, i.e., $T=T^*+\epsilon$, with $\epsilon\ll T^*$, then we know that the value of $x(T)$ will be just above $x(T^*)=x_+$ (to within order $\epsilon$). This implies that the switching time $t^*$ is given by

$$t^*=T+\frac{1}{2\beta}\ln\left[\frac{C}{\epsilon}\right], \tag{A11}$$

where $C$ is a constant that does not need to be specified. Here, a *logarithmic divergence* of the switching time is displayed, if the pulse duration just exceeds the critical one necessary to induce switching. This slowing-down phenomenon has a different behavior than the critical slowing down discussed before, as it is logarithmic instead of algebraic. It also has a different physical origin: it arises even if the device is not biased in the immediate vicinity of the switching points. *Noncritical slowing down* is physically due to the fact that the critical pulse duration brings the device right on the unstable state of the intermediate branch. This state, even though unstable, can accommodate the system for a finite time interval, even a long one. The two slowing-down mechanisms are displayed on the curves in Fig. 2. The large plateau is due to critical slowing down, while the subsequent (smaller) lethargy for a pulse duration (very) near the critical one is due to noncritical slowing down.


[1] H. G. Winful and G. D. Cooperman, Appl. Phys. Lett. **40**, 298 (1982).

[2] L. A. Lugiato, L. M. Narducci, D. K. Bandy, and C. A. Pennise, Opt. Commun. **43**, 281 (1982).

[3] H. G. Winful, R. Zamir, and S. Feldman, Appl. Phys. Lett. **58**, 1001 (1991).

[4] J. V. Moloney, IEEE J. Quantum Electron. **QE-21**, 1393 (1985).

[5] P. Mandel, Opt. Commun. **55**, 293 (1985).

[6] B. Segard, J. Zemmouri, and B. Macke, Opt. Commun. **60**, 323 (1986).

[7] J. Y. Bigot, A. Daunois, and P. Mandel, Phys. Lett. A **123**, 123 (1987).

[8] M. Haelterman, G. Vitrant, and R. Reinisch, J. Opt. Soc. Am. B **7**, 1309 (1990).

[9] L. A. Lugiato and C. Oldano, Phys. Rev. A **37**, 3896 (1988).

[10] M. Haelterman and G. Vitrant, J. Opt. Soc. Am. B **9**, 1563 (1992).

[11] L. A. Lugiato and R. Lefever, Phys. Rev. Lett. **58**, 2209 (1987); W. J. Firth, A. J. Scroggie, G. S. McDonald, and L. A. Lugiato, Phys. Rev. A **46**, 3609 (1992).

[12] J. Danckaert, Ph.D. thesis, Vrije Universiteit Brussel, Brussels, 1992 (unpublished).

[13] K. Ikeda, Opt. Commun. **30**, 257 (1979).

[14] E. Abraham and W. J. Firth, Opt. Acta **30**, 1541 (1983).

[15] A. A. Yefimov and G. N. Shkerdin, Sov. J. Commun. Technol. Electron. **36**, 59 (1991).

[16] P. Mandel, in *Optical Bistability, Instability and Optical Computing,* edited by H. Y. Zhang and K. K. Lee (World Scientific, Singapore, 1988), p. 118.